



Uzelac, Marina and Kennedy, Alan R. and Hernán-Gómez, Alberto and Fuentes, M. Ángeles and Hevia, Eva (2016) Heavier alkali-metal gallates as platforms for accessing functionalized abnormal NHC carbene-gallium complexes. Zeitschrift fur Anorganische und Allgemeine Chemie, 642 (22). pp. 1241-1244. ISSN 0044-2313 , <http://dx.doi.org/10.1002/zaac.201600310>

This version is available at <https://strathprints.strath.ac.uk/59256/>

Strathprints is designed to allow users to access the research output of the University of Strathclyde. Unless otherwise explicitly stated on the manuscript, Copyright © and Moral Rights for the papers on this site are retained by the individual authors and/or other copyright owners. Please check the manuscript for details of any other licences that may have been applied. You may not engage in further distribution of the material for any profitmaking activities or any commercial gain. You may freely distribute both the url (<https://strathprints.strath.ac.uk/>) and the content of this paper for research or private study, educational, or not-for-profit purposes without prior permission or charge.

Any correspondence concerning this service should be sent to the Strathprints administrator: strathprints@strath.ac.uk

Heavier alkali-metal gallates as platforms for accessing functionalized abnormal NHC carbene-gallium complexes

Marina Uzelac,^{*[a]} Alan R. Kennedy,^[a] Alberto Hernán-Gómez,^[a] M. Ángeles Fuentes^[a] and Eva Hevia^{*[a]}

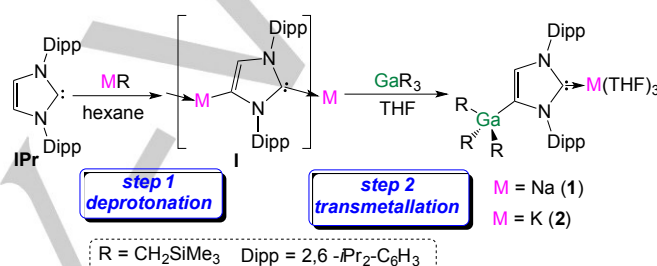
Abstract: By sequentially treating the unsaturated carbene IPr (IPr = 1,3-bis-(2,6-diisopropylphenyl)imidazol-2-ylidene) with heavier alkali-metal alkyls NaR or KR (R = CH₂SiMe₃) and GaR₃, novel heteroleptic gallates **1** and **2** have been prepared. Incorporating anionic NHC ligands, these bimetallic complexes react selectively with electrophiles to afford neutral abnormal NHC Ga complexes under mild conditions.

N-heterocyclic carbenes (NHCs), particularly imidazol-2-ylidenes, have played a pivotal role in advancing key areas of modern chemistry including transition-metal catalysis,^[1] stabilisation of low valent main-group compounds^[2] and the development of frustrated Lewis pair systems,^[3] to name just a few. By modifying the substituents on the N atoms or at the backbone of the imidazole ring, the electronic and steric properties of NHCs can be finely tune, making these commodity ligands extremely versatile.^[4,5] Typically imidazol-2-ylidenes bind to metal fragments through their C2 (normal) position although in some cases coordination can occur *via* a carbon from the imidazole backbone (C4 or abnormal coordination).^[4,5] NHCs can also exist as anionic moieties, as the result of their formal deprotonation, acting as a bridge between two metal centres employing simultaneously their C2 and C4 positions.^[6] Interestingly, Robinson has shown that electrophilic interception of anionic NHC complexes with MeOTf or HCl·NEt₃ can be employed to prepare abnormal NHC complexes (aNHCs) of B and Zn.^[7] More recently our group has also used a similar approach for the synthesis of aNHC complexes of Ga and Fe, where the normal C2 position of the carbene is blocked by a methyl group.^[8,9] Carbanionic NHCs can be prepared by several methods including chemical reduction and metal-mediated C-H activation, however deprotonative metallation appears to be one of the most versatile approaches.^[10]

The vast majority of the studies on NHC metallation have focussed on using organolithium reagents as a base,^[6,8] although mixed-metal systems such as zincates and magnesiates have shown great promise for the zincation or magnesiation of IPr (IPr = 1,3-bis-(2,6-diisopropylphenyl)imidazol-2-ylidene).^[11,12] Extending the scope of these investigations here we explore the metallating ability of heavier alkali-metal alkyls to prepare gallate complexes containing anionic NHC fragments and their applications to access novel aNHCs Ga complexes with a variety of substituents.

We started our studies by employing heavier alkali-metal alkyls

NaR and KR (R = CH₂SiMe₃) for direct metallation of IPr as this methodology seems to be underdeveloped. Treating a hexane suspension of IPr with MR (M = Na, K), led to the instant formation of yellow solids which were completely insoluble even when using large amounts of the more polar solvent THF. Interestingly, addition of GaR₃ solubilised these products allowing the isolation of heteroleptic alkali-metal gallates (THF)₃Na[C{[N(2,6-*i*-Pr₂C₆H₃)]₂CHCGa(CH₂SiMe₃)₃}] (**1**) and (THF)₃K[C{[N(2,6-*i*-Pr₂C₆H₃)]₂CHCGa(CH₂SiMe₃)₃}] (**2**) in 71 and 76% isolated yields respectively (Scheme 1).



Scheme 1. Stepwise indirect gallation of IPr affording alkali-metal gallates **1** and **2**.

Formation of gallates **1** and **2** can be rationalised in terms of a stepwise indirect gallation process. IPr is first deprotonated at the C4 position by the highly polar MR reagent (**I** in Scheme 1), which can then undergo fast transmetalation with the more electronegative Ga fragment, with the alkali-metal being trapped by the vacant C2 site of the carbene (Scheme 1). Although the solids obtained by treating IPr with MR cannot be characterised, due to their lack of solubility, the isolation of **1** and **2** provides compelling proof that these heavier alkaline metal alkyls can in fact metallate this NHC. Interestingly, when the single metal alkyl reagents are combined to form tetraorganogallates M₂GaR₄,^[13] the metallation process is inhibited yielding instead the coordination adducts [IPr₂K][GaR₄] (see SI for details) which highlights the potential of using bimetallic systems in a sequential manner.^[14] While the relevant M⁺IPr⁻ salts (**I**) are obtained via direct metallation, it should be noted that Goicoechea has structurally characterised K⁺IPr⁻·2THF as the result of the reaction of the lithiated IPr with potassium *tert*-butoxide.^[15]

Both sodium (**1**) and potassium gallate (**2**) exhibit discrete contacted ion-pair (CIP) structures where anionic NHC ligand coordinates to the alkali metal through its normal C2 position while Ga occupies the position previously filled by a H atom, bonding to the C4 position (Fig 1). The Ga-C4 distances (i.e. C24 for **1** and C2 for **2** in Fig 1) of 2.050(2) Å for **1** and 2.050(3) Å for **2** are close in value with the Ga-C_{alkyl} bonds (average 2.027 Å and 2.028 Å for **1** and **2** respectively) and they are also in excellent agreement with the bond distances found in the previously reported lithium congener.^[8] The narrow variation observed for the Ga-C bond lengths together with very similar

[a] M. Uzelac, Dr A. R. Kennedy, Dr A. Hernán-Gómez, Dr M. Á. Fuentes, Prof E. Hevia
WestCHEM, Department of Pure and Applied Chemistry
University of Strathclyde
Glasgow, G1 1XL (UK)
E-mail: eva.hevia@strath.ac.uk, marina.uzelac@strath.ac.uk

bond angles [mean angle 108.15° for **1** and 109.46° for **2**] reveal an almost ideal tetrahedral geometry of gallium centre in both compounds. With the virtually identical environment around Ga-atom, complexes **1** and **2** display their differences at the other end of the bridging ligand. Unsurprisingly, the M-C_{NHC} bond distance found in **1** [2.530(3) Å] is significantly shorter than that of **2** [2.902(3) Å], which is in agreement with the increase in size of the alkali-metal. Both values compare well with those reported for other anionic complexes containing these alkali-metals.^{19, 11, 13, 16, 17} Both sodium and potassium complete their coordination spheres by coordination of three molecules of THF, with more electropositive potassium gaining further stabilisation through electrostatic interaction with the *ipso* carbon of the pendant Dipp group on N2 (Figure 1). This secondary contact [K1...C16 = 3.301(3) Å] is within the range of previously reported potassium π -interactions¹⁸ and translates into a significantly more acute N2-C1-K1 angle ($107.77(18)^\circ$) than N1-C1-K1 ($150.71(19)^\circ$).

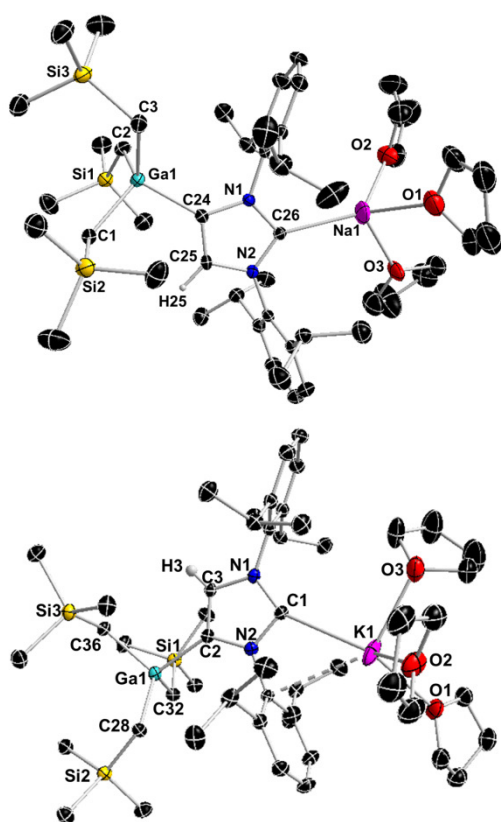
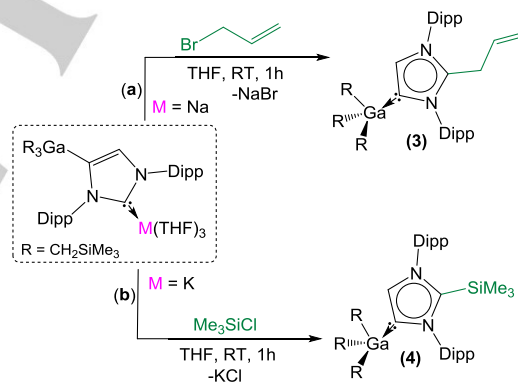


Figure 1. Molecular structure of **1** (top) and **2** (bottom) with 50% probability displacement ellipsoids. All hydrogen atoms except the one left on imidazole ring and disorder components in THF ligands have been omitted for clarity. Dashed lines represent secondary interactions.

From the NMR data of **1** and **2** in d_8 -THF solutions, the metallation of IPr is evident by the large downfield shift of the C4 resonance in the ^{13}C NMR spectra (from 122.3 in free IPr to 155.2 and 153.6 ppm respectively) as well as the presence of a diagnostic singlet integrating 1H in the ^1H NMR spectra for the imidazole CH (at 6.64 and 6.59 ppm respectively versus 7.19 in free IPr). The loss of symmetry in the imidazole ring is reflected

in the ^1H and ^{13}C NMR spectra with the appearance of two distinct sets of Dipp signals. In addition, the carbenic C atom attached to the alkali-metal can be observed at 202.8 and 210.7 ppm for **1** and **2** respectively, at similar values to those reported for other related complexes containing Na^[11] and K.^[15] The well-established notion that the size and the substitution pattern of the heterocyclic ring frame can have a large effect on the properties of carbene,^[18, 19] prompted us to investigate the potential of **1** and **2** as molecular synthons. To this end, **1** was reacted with an equimolar amount of allyl bromide and **2** with Me_3SiCl in THF at room temperature. In both cases the reaction proceeded with the formation of white precipitate (presumably alkali metal salts NaBr and KCl, respectively) affording $[\text{C}_3\text{H}_5\text{C}\{\text{N}(\text{2,6-}i\text{Pr}_2\text{C}_6\text{H}_3)_2\text{CHCGa}(\text{CH}_2\text{SiMe}_3)_3\}]$ (**3**) and $[\text{Me}_3\text{SiC}\{\text{N}(\text{2,6-}i\text{Pr}_2\text{C}_6\text{H}_3)_2\text{CHCGa}(\text{CH}_2\text{SiMe}_3)_3\}]$ (**4**) in 42 and 61 % yields respectively (Scheme 2). Compounds **3** and **4** are neutral abnormal NHC Ga complexes obtained as a result of the selective allylation (for **3**) and silylation (for **4**) of the C2 position of the anionic NHC ligand present in **1** and **2**, leaving the C4-Ga left intact. The isolation of **4** contrasts with the reactivity reported by Arnold for a related mixed K/Y complex,^[16] where the silylation occurs at the C4 position of the anionic carbene, instead of C2. Similar regioselectivity has been witnessed by Robinson for polymeric Li^+IPr^- , which in this case affords the C4-SiMe₃ substituted free carbene.^[6] Interestingly, by adding borane to this lithium complex, it is possible to direct the selectivity of the quench with SiMe_3Cl towards C2.^[7b]



Scheme 2. Electrophilic interception of anionic NHC complexes (a) **1** with allyl bromide and (b) **2** with Me_3SiCl .

The molecular structures of **3** and **4** have been established by X-ray crystallography (Fig 2). The Ga-C4 distances (i.e. C3 and C45 for **3** and **4** respectively) showed very little variation [2.0802(18) and 2.0887(16) Å] to that found in $[\text{aIPr-GaR}_3]$ ^[8] (2.0759(16) Å) where the C2 position of the carbene is occupied by a H atom, suggesting that the substituents on the C2 of the imidazole ring have little influence in the strength of the Ga-C4 bond. Another interesting trend is that despite the neutral constitution of these novel abnormal NHCs, the Ga-C bond distances are only slightly elongated to those discussed for the anionic precursors **1** and **2**. Structural analysis of **3** revealed it to be a cocrystal which contains $\text{CH}_2\text{-CH=CH}_2$ and CH=CH-CH_3 as substituents at the C2 of the carbene in approximately 2:3 ratio, arising from the partial allylic rearrangement. Mirroring this

composition in the solution, NMR spectroscopic analysis of **3** proved to be extremely complex in the allylic section (from 3 to 6 ppm); although it should be noted that no interconversion between these two isomers is observed over prolonged periods of time. Despite its complexity, the ^1H NMR spectrum displays four septets for the CH of isopropyl groups, while an informative resonance at 163.4 ppm is observed for the carbenic carbon. A similar chemical shift was observed for **4** (167.6 ppm) along with another signal at 148.8 ppm, which can be assigned to the C of the imidazole ring that is now bonded to a SiMe_3 group.

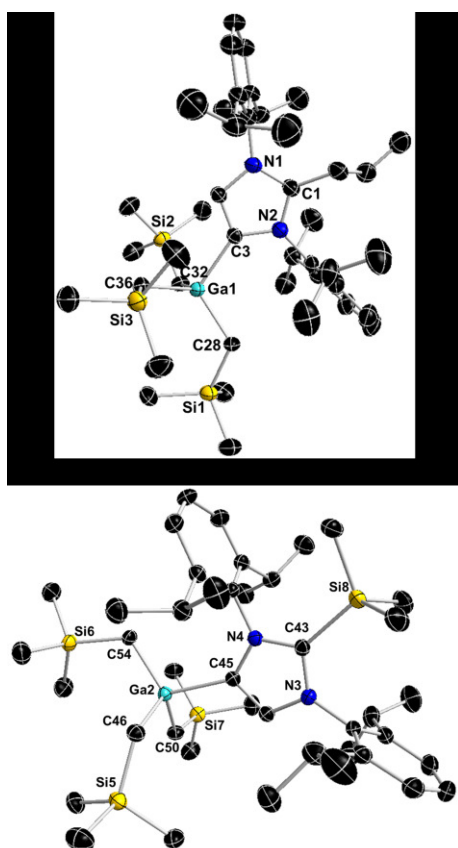


Figure 2. Molecular structure of **3** (top) and **4** (bottom) with 50% probability displacement ellipsoids. All hydrogen atoms have been omitted for clarity. For compound **3** only the $\text{CH}_2\text{-CH}=\text{CH}_2$ fragment is shown. The unit cell of **4** contains three crystallographically independent molecules with identical connectivity. One of these molecules is shown here.

Collectively these findings show the ability of heavier alkali metal alkyls to effectively metallate unsaturated NHC IPr when operating in tandem with a gallium alkyl, affording sodium and potassium gallate complexes **1** and **2** respectively. Electrophilic interception of these bimetallic compounds selectively yielded neutral abnormal Ga NHC complexes disclosing the preference of anionic ligand present in **1** and **2** to react with electrophiles via its C2 position while preserving the Ga-C4 bond.

Experimental Section

Full experimental details and copies of NMR spectra are included in the Supporting Information. CCDC 1501619-1501622 contain the

supplementary crystallographic data of this paper. These data can be obtained free of charge from the Cambridge Crystallographic Data Centre via www.ccdc.cam.ac.uk/data_request/cif.

Acknowledgements

We thank the European Research Council (ERC) for their generous sponsorship of this research.

Keywords: gallium • sodium • potassium • carbene ligands • coordination chemistry

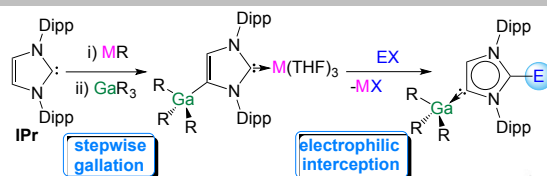
- [1] a) M. Scholl, S. Ding, C. W. Lee, R. H. Grubbs, *Org. Lett.* **1999**, *1*, 953-956; b) C. Valente, S. Calimsiz, K. H. Hoi, D. Mallik, M. Sayah, M. G. Organ, *Angew. Chem. Int. Ed.* **2012**, *51*, 3314-3332; *Angew. Chem.* **2012**, *124*, 3370-3388; c) S. Diez-Gonzalez, N. Marion, S. P. Nolan, *Chem. Rev.* **2009**, *109*, 3612-3676; d) D. Enders, O. Niemeier, A. Henseler, *Chem. Rev.* **2007**, *107*, 5606-5655.
- [2] a) Y. Wang, Y. Xie, P. Wei, R. B. King, H. F. Schaefer III, P. v. R. Schleyer, G. H. Robinson, *Science*, **2008**, *321*, 1069-1071; b) A. Sidiropoulos, C. Jones, A. Stasch, S. Klein, G. Frenking, *Angew. Chem. Int. Ed.* **2009**, *48*, 9701-9704; *Angew. Chem.* **2009**, *121*, 9881-9884; c) R. S. Ghadwal, H. W. Roesky, S. Merkel, J. Henn, D. Stalke, *Angew. Chem. Int. Ed.* **2009**, *48*, 5683-5686; *Angew. Chem.* **2009**, *121*, 5793-5796; d) C. Jones, A. Sidiropoulos, N. Holzmann, G. Frenking, A. Stasch, *Chem. Commun.* **2012**, *48*, 9855-9857; e) Y. Wang, Y. Xie, P. Wei, R. B. King, H. F. Schaefer III, P. v. R. Schleyer, G. H. Robinson, *J. Am. Chem. Soc.* **2008**, *130*, 14970-14971; f) M. Y. Abraham, Y. Wang, Y. Xie, P. Wei, H. F. Schaefer III, P. v. R. Schleyer, G. H. Robinson, *Chem. Eur. J.* **2010**, *16*, 432-435; g) H. Braunschweig, R. D. Dewhurst, K. Hammond, J. Mies, K. Radacki, A. Vargas, *Science* **2012**, *336*, 1420-1422.
- [3] a) L. J. Hounjet, D. W. Stephan, *Org. Process Res. Dev.* **2014**, *18*, 385-391; b) D. W. Stephan, *Acc. Chem. Res.* **2015**, *48*, 306-316; c) M. Tamm in *Frustrated Lewis Pair I: Uncovering and Understanding* (Eds.: G. Erker, D. W. Stephan), Springer, **2013**, pp 121-155.
- [4] a) M. Albrecht, *Chem. Commun.* **2008**, 3601-3610; b) O. Schuster, L. Yang, H. Raubenheimer, M. Albrecht, *Chem. Rev.* **2009**, *109*, 3445-3478; c) M. Albrecht, *Science* **2009**, *326*, 532-533.
- [5] R. H. Crabtree, *Coord. Chem. Rev.* **2013**, *257*, 755-766.
- [6] Y. Wang, Y. Xie, M. Y. Abraham, P. Wei, H. F. Schaefer III, P. v. R. Schleyer, G. H. Robinson, *J. Am. Chem. Soc.* **2010**, *132*, 14370-14372.
- [7] a) Y. Wang, Y. Xie, M. Y. Abraham, R. G. Gilliard Jr., P. Wei, C. F. Campana, H. F. Schaefer III, P. v. R. Schleyer, G. H. Robinson, *Angew. Chem. Int. Ed.* **2012**, *51*, 10173-10176; *Angew. Chem.* **2012**, *124*, 10320-10323; b) Y. Wang, M. Y. Abraham, R. G. Gilliard Jr., P. Wei, J. C. Smith, G. H. Robinson, *Organometallics* **2012**, *31*, 791-793; c) M. Chen, Y. Wang, R. J. Gilliard Jr., P. Wei, N. A. Schwartz, G. H. Robinson, *Dalton Trans.* **2014**, *43*, 14211-14214.
- [8] M. Uzelac, A. Hernán-Gómez, D. R. Armstrong, A. R. Kennedy, E. Hevia, *Chem. Sci.* **2015**, *6*, 5719-5728.
- [9] L. C. H. Maddock, T. Cadenbach, A. R. Kennedy, I. Borilovic, G. Aromí, E. Hevia, *Inorg. Chem.* **2015**, *54*, 9201-9210.
- [10] J. B. Waters, J. M. Goicoechea, *Coord. Chem. Rev.* **2015**, *293-294*, 80-94.
- [11] D. R. Armstrong, S. E. Baillie, V. L. Blair, N. G. Chablocz, J. Diez, J. Garcia-Alvarez, A. R. Kennedy, S. D. Robertson, E. Hevia, *Chem. Sci.* **2013**, *4*, 4259-4266.
- [12] A. J. Martínez-Martínez, M. Ángeles Fuentes, A. Hernán-Gómez, E. Hevia, A. R. Kennedy, R. E. Mulvey, C. T. O'Hara, *Angew. Chem. Int. Ed.* **2015**, *54*, 14075-14079; *Angew. Chem.* **2015**, *127*, 14281-14285.
- [13] D. R. Armstrong, E. Brammer, T. Cadenbach, E. Hevia, A. R. Kennedy, *Organometallics* **2013**, *32*, 480-489.

- [14] a) D. R. Armstrong, E. Crosbie, E. Hevia, R. E. Mulvey, D. L. Ramsay, S. D. Robertson, *Chem. Sci.* **2014**, *5*, 3031-3045; b) W. Clegg, E. Crosbie, S. H. Dale-Black, E. Hevia, G. Honeyman, A. R. Kennedy, R. E. Mulvey, D. L. Ramsay, S. D. Robertson, *Organometallics* **2015**, *34*, 2580-2589.
- [15] J. B. Waters, J. M. Goicoechea, *Dalton. Trans.* **2014**, *43*, 14239-14248.
- [16] P. L. Arnold, S. T. Liddle, *Organometallics* **2006**, *25*, 1485-1491.
- [17] P. K. Majhi, G. Schnakenburg, Z. Kelemen, L. Nyulaszi, D. P. Gates, R. Streibel, *Angew. Chem. Int. Ed.* **2013**, *52*, 10080-10083; *Angew. Chem.* **2013**, *125*, 10264-10267.
- [18] a) F. Feil, S. Harder, *Organometallics* **2000**, *19*, 5010-5015; b) G. C. Forbes, A. R. Kennedy, R. E. Mulvey, B. A. Roberts, R. B. Rowling, *Organometallics* **2002**, *21*, 5115-5121; c) K. L. Hull, I. Carmichael, B. C. Noll, K. W. Henderson, *Chem. Eur. J.* **2008**, *14*, 3939-3953; d) M. Uzelac, I. Borilovic, M. Amores, T. Cadenbach, A. R. Kennedy, G. Aromí, E. Hevia, *Chem. Eur. J.* **2016**, *22*, 4843-4854; d) M. S. Hill, G. Kociok-Köhn, D. J. MacDougall, *Inorg. Chem.* **2011**, *50*, 5234-5241; e) M. I. Lipschutz, T. Chantarojsiri, Y. Dong, T. D. Tilley, *J. Am. Chem. Soc.* **2015**, *137*, 6336-6372.
- [19] M. N. Hopkinson, C. Richter, M. Schedler, F. Glorius, *Nature*, **2014**, *510*, 485-496.
- [20] D. Mendoza-Espinosa, B. Donnadiou, G. Bertrand, *J. Am. Chem. Soc.* **2010**, *132*, 7264-7265.

Entry for the Table of Contents (Please choose one layout)

Layout 2:

COMMUNICATION



*M. Uzelac, * A. R. Kennedy, A. Hernán-Gómez, M. Á. Fuentes, E. Hevia**

Page No. – Page No.

Heavier alkali-metal gallates as platforms for accessing functionalised abnormal NHC-gallium complexes

Electrophilic interception of alkali-metal gallates, obtained using by indirect gallation of IPr has revealed a versatile method to access C2-substituted abnormal NHC Ga complexes

Additional Author information for the electronic version of the article.

Author: ORCID identifier
Author: ORCID identifier
Author: ORCID identifier

WILEY-VCH

SUPPORTING INFORMATION

Title: Heavier Alkali-metal Gallates as Platforms for Accessing Functionalized Abnormal NHC Carbene-Gallium Complexes

Author(s): M. Uzelac,* A. R. Kennedy, A. Hernán-Gómez, M. Á. Fuentes, E. Hevia*

Ref. No.: Z.201600310

Heavier alkali-metal NHC gallates as platforms for accessing functionalized abnormal carbene-gallium complexes

Marina Uzelac,^{*,[a]} Alan R. Kennedy,^[a] Alberto Hernán-Gómez,^[a] M. Ángeles Fuentes^[a] and Eva Hevia^{*,[a]}

WestCHEM, Department of Pure and Applied Chemistry, University of Strathclyde, 295 Cathedral Street, Glasgow, G1 1XL, UK

eva.hevia@strath.ac.uk

marina.uzelac@strath.ac.uk

Contents

General experimental details.....	2
X-Ray Crystallography	2
Synthesis of products	3
Representative reaction of alkali-metal gallate with IPr	6
NMR spectra	7

General experimental details

All reactions were carried out using standard Schlenk and glove box techniques under an inert atmosphere of argon. Solvents (THF, hexane, benzene and toluene) were dried by heating to reflux over sodium benzophenone ketyl and distilled under nitrogen prior to use. NMR spectra were recorded on a Bruker DPX 400 MHz spectrometer, operating at 400.13 MHz for ^1H , and 100.62 MHz for $^{13}\text{C}\{^1\text{H}\}$. Elemental analyses were obtained using a Perkin Elmer 2400 elemental analyser. Allyl bromide was purchased from Sigma Aldrich Chemicals and used as received. Me_3SiCl was purchased from Sigma Aldrich Chemicals, dried over calcium hydride and stored over 4 Å molecular sieves prior to use. $[\text{Ga}(\text{CH}_2\text{SiMe}_3)_3]$,¹ $[\text{NaCH}_2\text{SiMe}_3]$,² $[\text{KCH}_2\text{SiMe}_3]$ ^{2a,3} and IPr^4 were prepared according to literature methods.

X-Ray Crystallography

Crystallographic data for **2**, **3** and **4** were measured at 123(2) K with an Oxford Diffraction Gemini S instrument with graphite-monochromated Cu ($\lambda=1.54180$ Å) radiation. For **1** an Oxford Diffraction Xcalibur E instrument and Mo ($\lambda=0.71073$ Å) radiation was used. All structures were refined to convergence on F^2 using all unique reflections and programs from the SHELX family.⁵ The final model for all structures included constraints and restraints on bond lengths and displacement parameters that were required to model disordered groups. THF ligands (for **1** and **2**) and three SiMe_3 groups of **4** were modelled as disordered over two sites. For **3** several different models were investigated. The final model for the alkene fragment contained disordered $\text{CH}_2\text{-CH=CH}_2$ (40.8 %) and CH=CH-CH_3 (59.2 %) fragments and three separate disorder components. Selected crystallographic data are presented in Table S1 and full details in cif format can be obtained free of charge from the Cambridge Crystallographic Data Centre via www.ccdc.cam.ac.uk/data_request/cif.

Table S1: Selected crystallographic and refinement parameters for compounds **1-4**.

Compound	1	2	3	4
Empirical formula	$\text{C}_{51}\text{H}_{92}\text{GaN}_2\text{NaO}_3\text{Si}_3$	$\text{C}_{51}\text{H}_{92}\text{GaKN}_2\text{O}_3\text{Si}_3$	$\text{C}_{42}\text{H}_{73}\text{GaN}_2\text{Si}_3$	$\text{C}_{42}\text{H}_{77}\text{GaN}_2\text{Si}_4$
Formula weight	958.24	974.35	760.01	792.13
Crystal system	Triclinic	Triclinic	Orthorhombic	Monoclinic
Space group	P -1	P -1	P bca	P 2 ₁ /c
χ (Å)	0.71073	1.5418	1.5418	1.5418
a (Å)	10.7828(8)	10.8225(4)	15.7786(2)	16.02200(10)
b (Å)	14.5956(9)	14.8126(4)	18.2659(2)	48.5616(3)
c (Å)	19.1526(12)	19.1585(7)	31.7708(5)	18.64600(10)
α (°)	97.397(5)	99.854(3)	90	90
β (°)	95.292(6)	94.205(3)	90	96.3220(10)

¹ L. M. Dennis, W. Patnode, *J. Am. Chem. Soc.* **1932**, 54, 182.

² a) A. J. Hart, D. H. O'Brien, C. R. Russell, *J. Organomet Chem.* **1974**, 72, C19; b) W. Clegg, B. Conway, A. R. Kennedy, J. Klett, R. E. Mulvey, L. Russo, *Eur. J. Inorg. Chem.* **2011**, 721.

³ B. Conway, D. V. Graham, E. Hevia, A. R. Kennedy, J. Klett, R. E. Mulvey, *Chem. Commun.* **2008**, 2638.

⁴ L. Hintermann, *Beilstein Journal of Organic Chemistry* **2007**, 3, 1.

⁵ G. M. Sheldrick, *Acta Crystallogr.*, **2008**, A64, 112.

γ (°)	105.058(6)	104.535(3)	90	90
V (Å ³)	2861.6(3)	2907.28(18)	9156.7(2)	14419.37(17)
Z	2	2	8	12
μ (mm ⁻¹)	0.589	2.160	1.771	1.934
2 θ max (°)	54.994	146.792	146.484	146.57
Measured reflections	27405	22187	41291	163145
Unique reflections	13103	11344	9105	28653
Observed reflections	9034	9125	7610	24954
R _{int}	0.0523	0.0567	0.0405	0.0345
R [on F, obs refln only]	0.0538	0.0661	0.0391	0.0411
wR [on F ² , all data]	0.1197	0.1792	0.1064	0.1079
GoF	1.019	1.027	1.024	1.029
Largest diff peak/hole (e Å ⁻³)	0.614/-0.811	1.504/-0.487	0.367/-0.213	0.951/-0.313

Synthesis of products

Synthesis of (THF)₃Na[C{[N(2,6-ⁱPr₂C₆H₃)₂CHCGa(CH₂SiMe₃)₃}] (1)

Equimolar amounts of Na(CH₂SiMe₃) (0.22g, 2 mmol) and IPr (0.8 g, 2 mmol) were suspended in hexane (10 mL) and stirred for 2h at room temperature. To the obtained slurry, a hexane solution of Ga(CH₂SiMe₃)₃ (0.66 g, 2 mmol in 10 mL hexane) was added via cannula and stirred over night at room temperature. The reaction mixture was then concentrated to approximately 5 mL and 1 mL of THF was added to afford a straw solution. Overnight storage of the solution at -30 °C provided a batch of colourless crystals (1.36 g, 71 %). It should be noted that two coordinated THF molecules are lost upon drying in vacuo. Anal. Calcd for C₄₃H₇₆N₂Si₃NaOGa: C, 63.44; H, 9.41; N, 3.44. Found: C, 63.21; H, 9.44; N, 3.70.

¹H NMR (298 K, C₆D₆) δ (ppm) -0.62 (6H, s, CH₂SiMe₃), 0.37 (27H, s, Si(CH₃)₃), 1.04 (12H, d, CH(CH₃)₂), 1.31 (20H, mult, CH(CH₃)₂ + THF), 1.57 (6H, d, CH(CH₃)₂), 3.00 (2H, sept, CH(CH₃)₂), 3.09 (14H, mult, THF), 3.21 (2H, sept, CH(CH₃)₂), 6.99 (1H, s, imidazole backbone CH), 7.08 (2H, p-CH), 7.16-7.21 (4H, mult, m-CH overlapping with C₆D₆).
¹³C{¹H} NMR (298 K, C₆D₆) δ (ppm) 0.2 (CH₂SiMe₃), 3.8 (Si(CH₃)₃), 23.3 (CH(CH₃)₂), 24.8 (CH(CH₃)₂), 25.3 (CH(CH₃)₂), 25.5 (CH(CH₃)₂), 27.9 (CH(CH₃)₂), 28.1 (CH(CH₃)₂),

123.4 (Ar-CH), 123.7 (Ar-CH), 124.5 (Ar-CH), 128.5 (Ar-CH), 129.2 (imidazole backbone CH), 139.1 (Ar-C), 142.7 (Ar-C), 146.8 (Ar-C), 146.9 (Ar-C), 156.0(C-Ga), 198.6 (C:).

^1H NMR (298 K, d_8 -THF) $\delta(\text{ppm})$ -1.18 (6H, s, CH_2SiMe_3), -0.17 (27H, s, $\text{Si}(\text{CH}_3)_3$), 1.09-1.19 (12H, mult, $\text{CH}(\text{CH}_3)_2$), 1.30 (6H, d, $\text{CH}(\text{CH}_3)_2$), 3.0 (4H, mult, $\text{CH}(\text{CH}_3)_2$), 6.64 (1H, s, imidazole backbone CH), 7.18-7.36 (6H, mult, m-CH + p-CH). **$^{13}\text{C}\{^1\text{H}\}$ NMR (298 K, d_8 -THF) $\delta(\text{ppm})$** 0.2 (CH_2SiMe_3), 3.7 ($\text{Si}(\text{CH}_3)_3$), 23.3 ($\text{CH}(\text{CH}_3)_2$), 25.1 ($\text{CH}(\text{CH}_3)_2$), 25.3 ($\text{CH}(\text{CH}_3)_2$), 26.4 ($\text{CH}(\text{CH}_3)_2$), 28.5 ($\text{CH}(\text{CH}_3)_2$), 28.6 ($\text{CH}(\text{CH}_3)_2$), 123.6 (Ar-CH), 124.1 (Ar-CH), 127.9 (Ar-CH), 128.8 (Ar-CH), 129.5 (imidazole backbone CH), 139.1 (Ar-C), 142.7 (Ar-C), 147.3 (Ar-C), 147.5 (Ar-C), 155.2 (C-Ga), 202.8 (C:).

Synthesis of $(\text{THF})_3\text{K}[\text{C}\{[\text{N}(2,6\text{-}^i\text{Pr}_2\text{C}_6\text{H}_3)]_2\text{CHCGa}(\text{CH}_2\text{SiMe}_3)_3\}]$ (**2**)

Equimolar amounts of $\text{K}(\text{CH}_2\text{SiMe}_3)$ (0.26 g, 2 mmol) and IPr (0.8 g, 2 mmol) were suspended in hexane (10 mL) and stirred for 2h at room temperature. To the obtained slurry, a hexane solution of $\text{Ga}(\text{CH}_2\text{SiMe}_3)_3$ (0.66 g, 2 mmol in 10 mL hexane) was added via cannula and stirred over night at room temperature. The reaction mixture was then concentrated to approximately 5 mL and 1 mL of THF was added to afford a straw solution. Overnight storage of the solution at $-30\text{ }^\circ\text{C}$ provided a batch of colourless crystals (1.48 g, 76 %). It should be noted that one coordinated THF molecule is lost upon drying in vacuo. Anal. Calcd for $\text{C}_{47}\text{H}_{84}\text{N}_2\text{Si}_3\text{KO}_2\text{Ga}$: C, 62.57; H, 9.38; N, 3.10. Found: C, 62.71; H, 9.62; N, 3.45 %).

^1H NMR (298 K, d_8 -THF) $\delta(\text{ppm})$ -1.16 (6H, s, CH_2SiMe_3), -0.17 (27H, s, $\text{Si}(\text{CH}_3)_3$), 1.09 (12H, d, $\text{CH}(\text{CH}_3)_2$), 1.17 (6H, d, $\text{CH}(\text{CH}_3)_2$), 1.29 (6H, d, $\text{CH}(\text{CH}_3)_2$), 3.02 (4H, mult, $\text{CH}(\text{CH}_3)_2$), 6.59 (1H, s, imidazole backbone CH), 7.15-7.28 (6H, mult, m-CH + p-CH). **$^{13}\text{C}\{^1\text{H}\}$ NMR (298 K, d_8 -THF) $\delta(\text{ppm})$** 0.2 (CH_2SiMe_3), 3.7 ($\text{Si}(\text{CH}_3)_3$), 23.2 ($\text{CH}(\text{CH}_3)_2$), 24.9 ($\text{CH}(\text{CH}_3)_2$), 25.3 ($\text{CH}(\text{CH}_3)_2$), 26.4 ($\text{CH}(\text{CH}_3)_2$), 28.4 ($\text{CH}(\text{CH}_3)_2$), 28.6 ($\text{CH}(\text{CH}_3)_2$), 123.2 (Ar-CH), 123.7 (Ar-CH), 127.6 (Ar-CH), 128.2 (Ar-CH), 128.6 (imidazole backbone CH), 140.8 (Ar-C), 144.3 (Ar-C), 147.3 (Ar-C), 147.4 (Ar-C), 153.6 (C-Ga), 210.7 (C:).

Synthesis of $[\text{C}_3\text{H}_5\text{C}\{[\text{N}(2,6\text{-}^i\text{Pr}_2\text{C}_6\text{H}_3)]_2\text{CHCGa}(\text{CH}_2\text{SiMe}_3)_3\}]$ (**3**)

To a THF solution of **1** (0.48 g, 0.5 mmol in 5 mL of THF) allyl bromide (0.06 g, 43 μL , 0.5 mmol) was added inducing precipitation. Obtained suspension was stirred for 1h at room

temperature and then filtered through Celite. Orange filtrate was layered with 3 mL of hexane and stored at -33 °C to afford colourless crystals of title compound (0.16 g, 42%). Anal. Calcd. for C₄₂H₇₃N₂Si₃Ga: C, 66.37; H, 9.68; N, 3.69. Found: C, 65.69; H, 9.66; N, 3.84. The NMR analysis is very complex and the reported chemical shifts are for both CH=CH-CH₃ and CH₂-CH=CH₂ fragments.

¹H NMR (298 K, d₈-THF) δ(ppm) -0.67 (6H, mult, CH₂SiMe₃), -0.29 and -0.33 (27H, s, Si(CH₃)₃), 0.81-1.46 (24H, mult, CH(CH₃)₂), 2.35(0.8 H, mult, CH(CH₃)₂), 2.51(1.2 H, mult, CH(CH₃)₂), 2.70(0.8 H, mult, CH(CH₃)₂), 2.85 (1.2 H, mult, CH(CH₃)₂), 2.95 (0.5 H, d, CH=CH-CH₃), [4.12, 4.36, 4.54, 4.67, 5.00, 5.60] (CH₂-CH=CH₂ + CH=CH-CH₃), 6.88 (7H, mult, imidazole backbone CH + Ar-CH), **¹³C{¹H} NMR (298 K, d₈-THF) δ(ppm)** 0.3 (CH₂SiMe₃), 3.6 (Si(CH₃)₃), 22.6 (CH(CH₃)₂), 22.8(CH(CH₃)₂), 23.0(CH(CH₃)₂), 23.7(CH(CH₃)₂), 23.8(CH(CH₃)₂), 23.9(CH(CH₃)₂), 24.4(CH(CH₃)₂), 24.5(CH(CH₃)₂), 24.6(CH(CH₃)₂), 26.4(CH(CH₃)₂), 28.3(CH(CH₃)₂), 28.4(CH(CH₃)₂), 28.5(CH(CH₃)₂), 28.7(CH(CH₃)₂), 30.1 (CH=CH-CH₃), [114.2, 115.9, 120.3, 124.1, 124.4, 124.6, 124.7, 124.8, 125.1 CH₂-CH=CH₂ + CH=CH-CH₃], [130.1, 130.2, 130.5, 130.8, 130.9, 131.2, 131.4, 131.7 aromatic CH + imidazole backbone CH], [134.1, 134.7, 136.6 Ar-C], 141.6 (C2-C), [143.7, 145.5, 145.6, 145.7 Ar-C], 163.4 (C-Ga).

Synthesis of [Me₃SiC{[N(2,6-ⁱPr₂C₆H₃)]₂CHCGa(CH₂SiMe₃)₃}] (**4**)

To a THF solution of **2** (0.49 g, 0.5 mmol in 5 mL of THF) dried TMSCl (0.05 g, 63 μL, 0.5 mmol) was inducing precipitation. Obtained suspension was stirred for 1h at room temperature and then filtered through Celite. Clear filtrate was layered with 2 mL of hexane and stored at -33 °C to afford colourless crystals of title compound (0.24 g, 61%). Anal. Calcd for C₄₂H₇₇N₂Si₄Ga: C, 63.68; H, 9.80; N, 3.54. Found: C, 62.89; H, 9.46; N, 3.60.

¹H NMR (298 K, C6D6) δ(ppm) -0.69 (6H, s, CH₂SiMe₃), -0.46 (9H, s, SiCH₃), 0.33 (27H, s, Si(CH₃)₃), 1.03 (6H, d, CH(CH₃)₂), 1.09 (12H, d, CH(CH₃)₂), 1.40 (6H, d, CH(CH₃)₂), 2.40 (2H, sept, CH(CH₃)₂), 2.76 (2H, sept, CH(CH₃)₂), 6.95 (2H, d, Ar-CH), 7.04 (2H, d, Ar-CH), 7.12-7.21 (3H, mult, Ar-CH + CH imidazole backbone). **¹³C{¹H} NMR (298 K, d₈-THF) δ(ppm)** -0.5 (SiCH₃), 1.3 (CH₂SiMe₃), 3.7 (Si(CH₃)₃), 21.6 (CH(CH₃)₂), 24.3 (CH(CH₃)₂), 25.1 (CH(CH₃)₂), 28.0 (CH(CH₃)₂), 28.5 (CH(CH₃)₂), 28.9 (CH(CH₃)₂), 124.2

(Ar-CH), 124.4 (Ar-CH), 130.5 (Ar-CH), 131.4 (Ar-CH), 133.1 (Ar-C), 135.3 (imidazole backbone CH), 137.3 (Ar-C), 145.3 (Ar-C), 146.5 (Ar-C), 148.8 (C-SiMe₃), 167.6 (C-Ga).

Representative reaction of alkali-metal gallate with IPr

To a hexane suspension of KGaR₄ (R = CH₂SiMe₃) an equivalent of IPr was added via solid addition tube and the obtained suspension stirred at room temperature for 1h. The suspension was gently heated until the solution was obtained which upon cooling produced colourless crystals. The multinuclear NMR spectroscopic analysis of crystals reveals no deprotonation of the backbone and suggests formation of ligand separated potassium gallate [$\{K(IPr)_2\}^+\{Ga(CH_2SiMe_3)_4\}^-$].

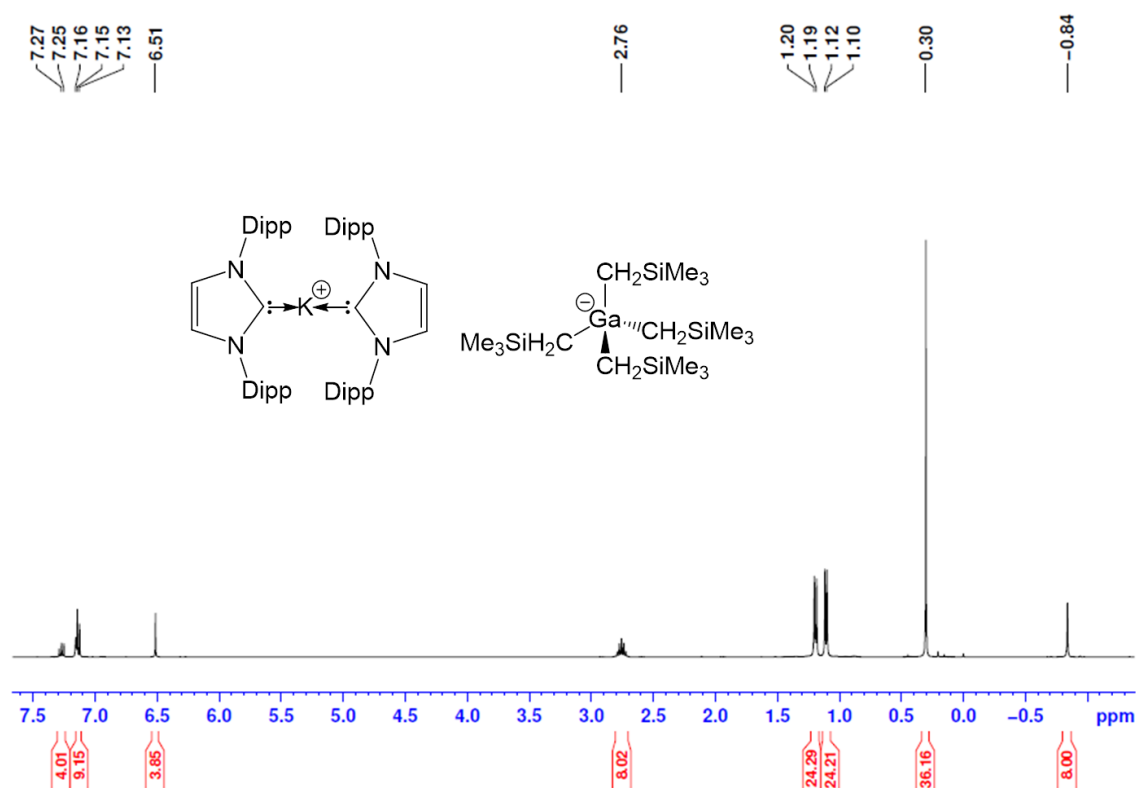


Figure S1: ¹H NMR spectrum of [$\{K(IPr)_2\}^+\{Ga(CH_2SiMe_3)_4\}^-$] in C₆D₆.

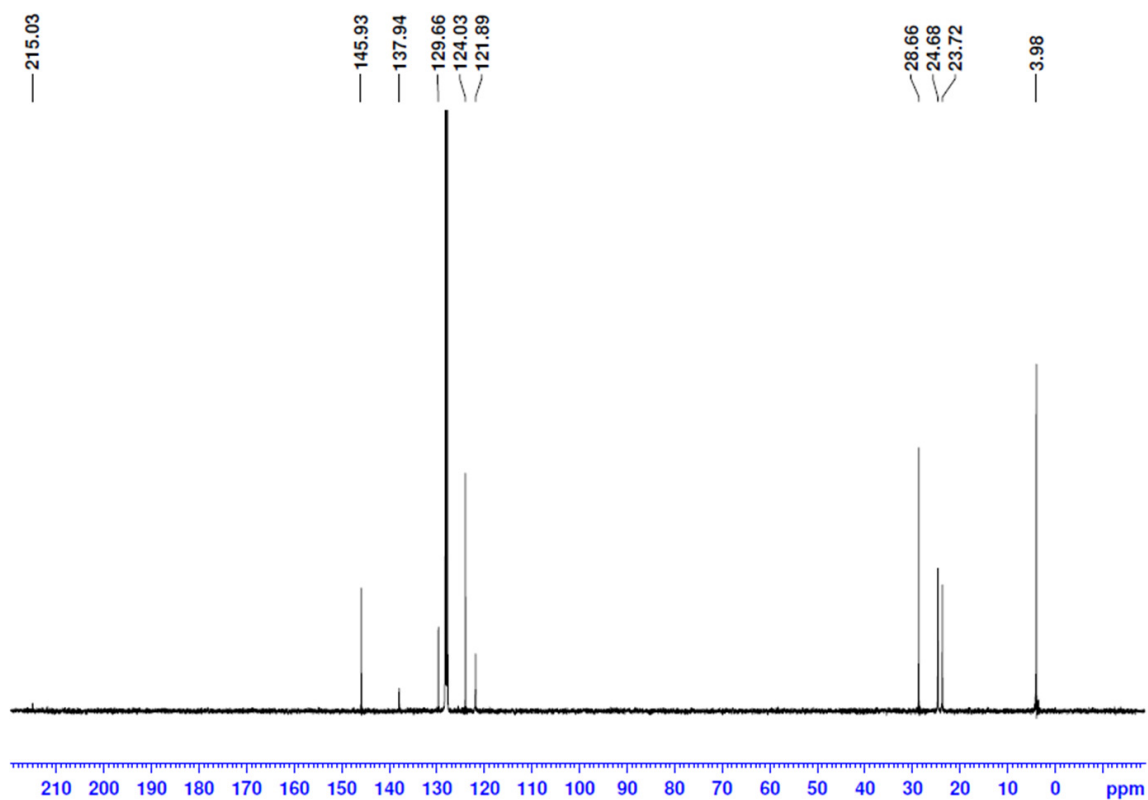


Figure S2: ^{13}C NMR spectrum of $[\{\text{K}(\text{IPr})_2\}^+\{\text{Ga}(\text{CH}_2\text{SiMe}_3)_4\}]$ in C_6D_6 .

NMR spectra

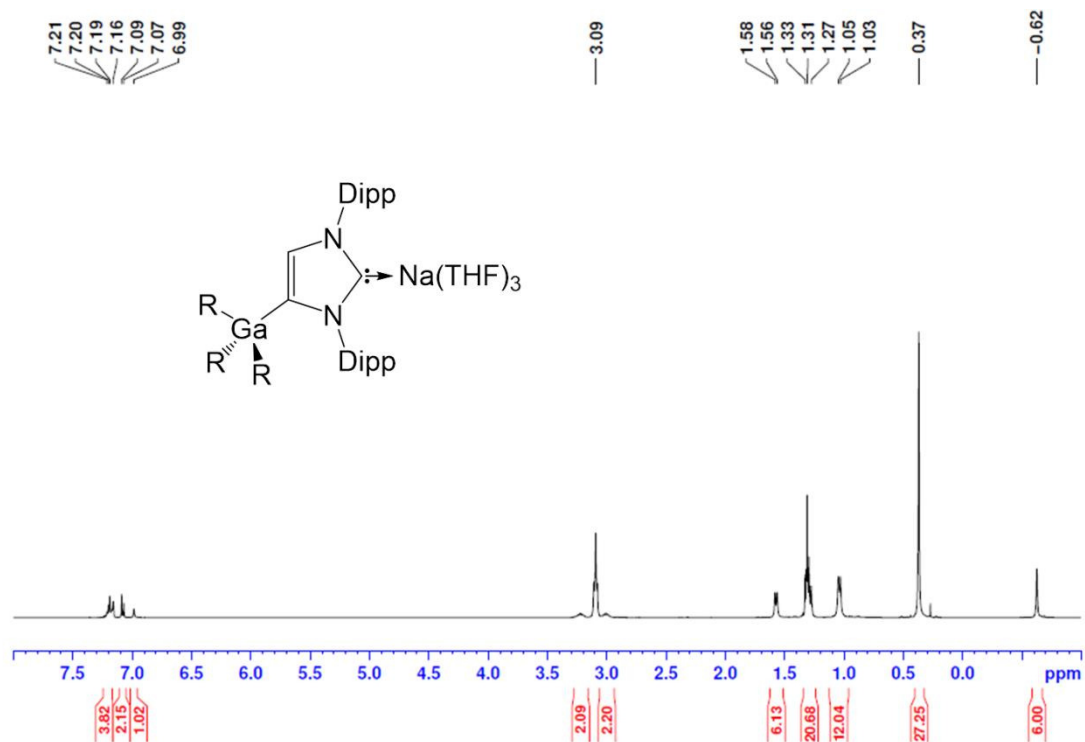
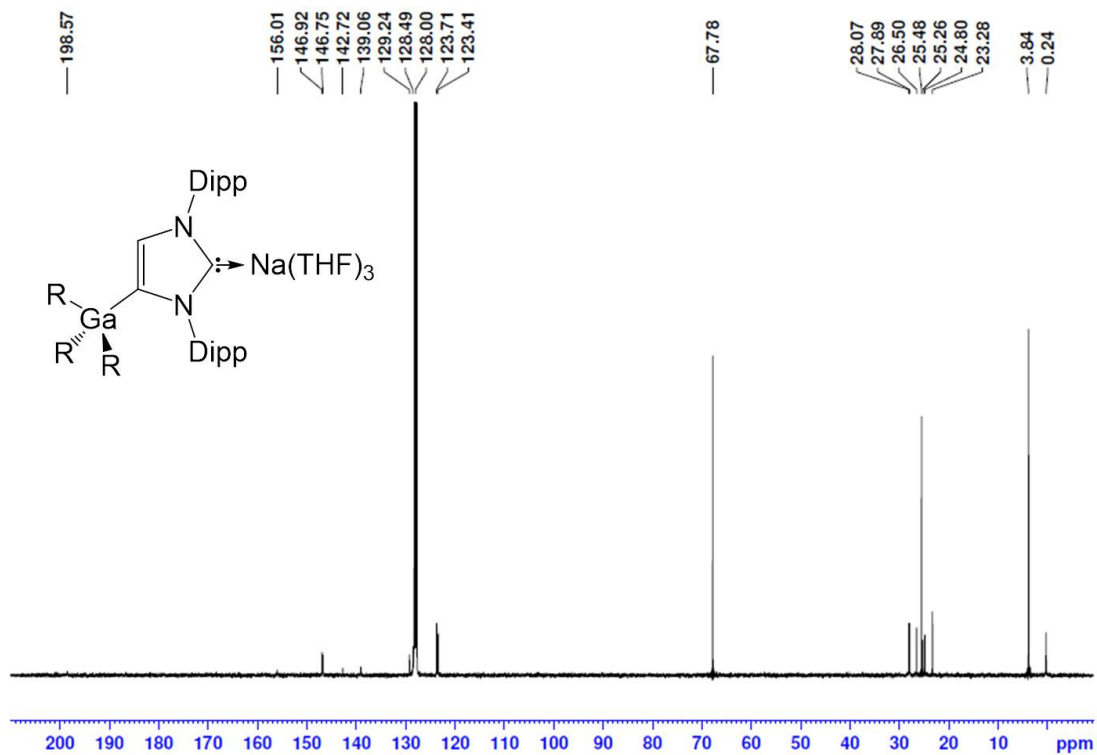
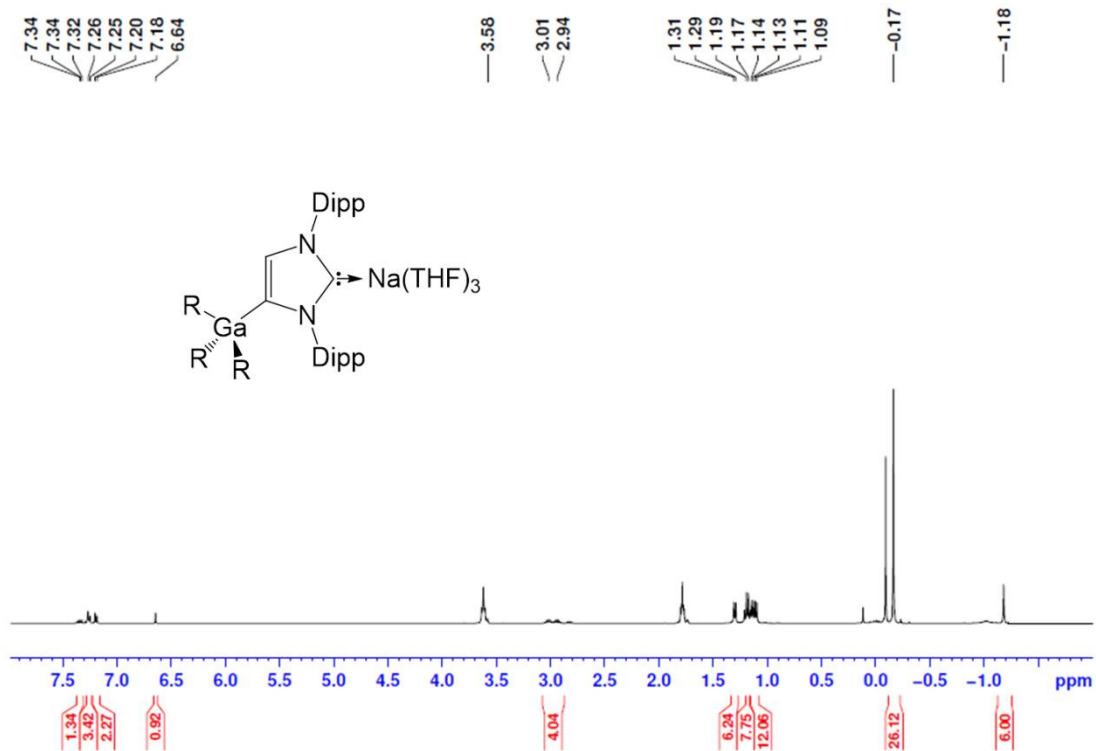


Figure S3: ^1H NMR spectrum of **1** in C_6D_6 .**Figure S4:** ^{13}C NMR spectrum of **1** in C_6D_6 .**Figure S5:** ^1H NMR spectrum of **1** in $\text{d}_8\text{-THF}$.

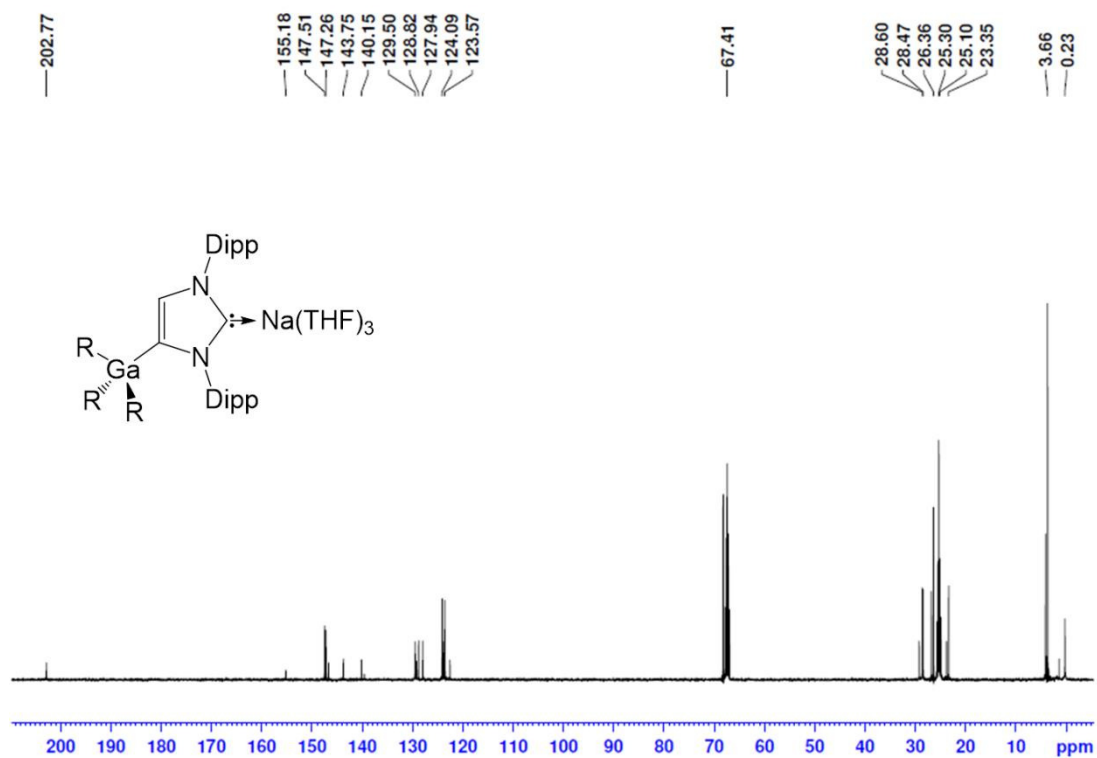


Figure S6: ¹³C NMR spectrum of **1** in d₈-THF.

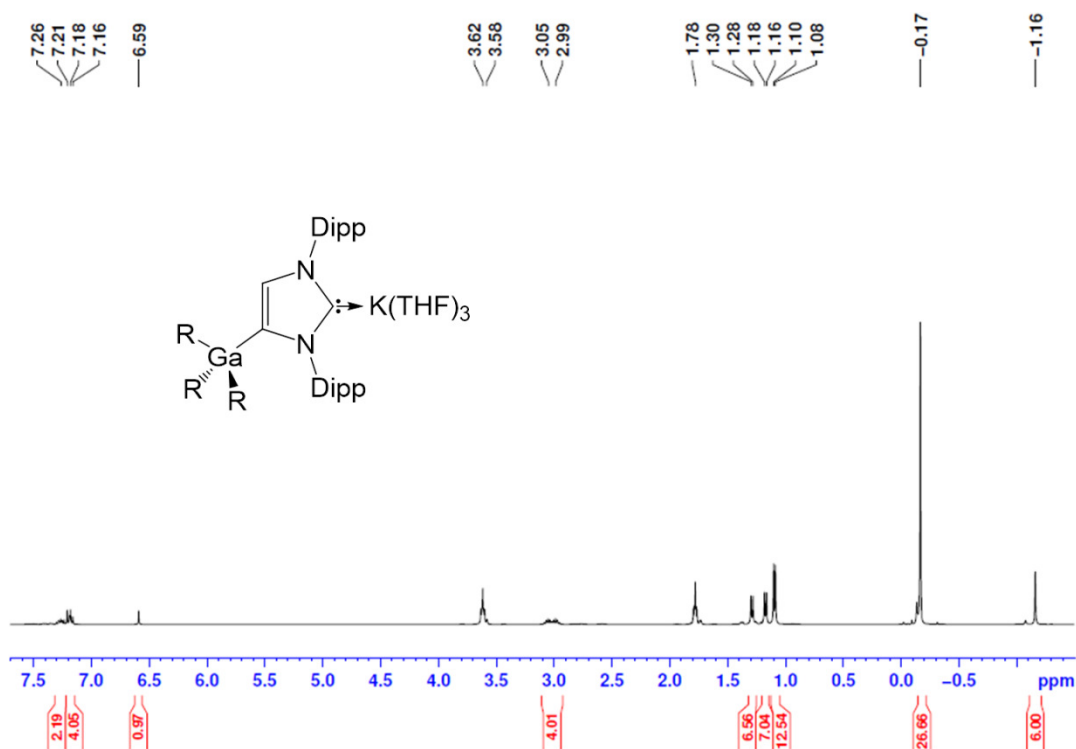


Figure S7: ¹H NMR spectrum of **2** in d₈-THF.

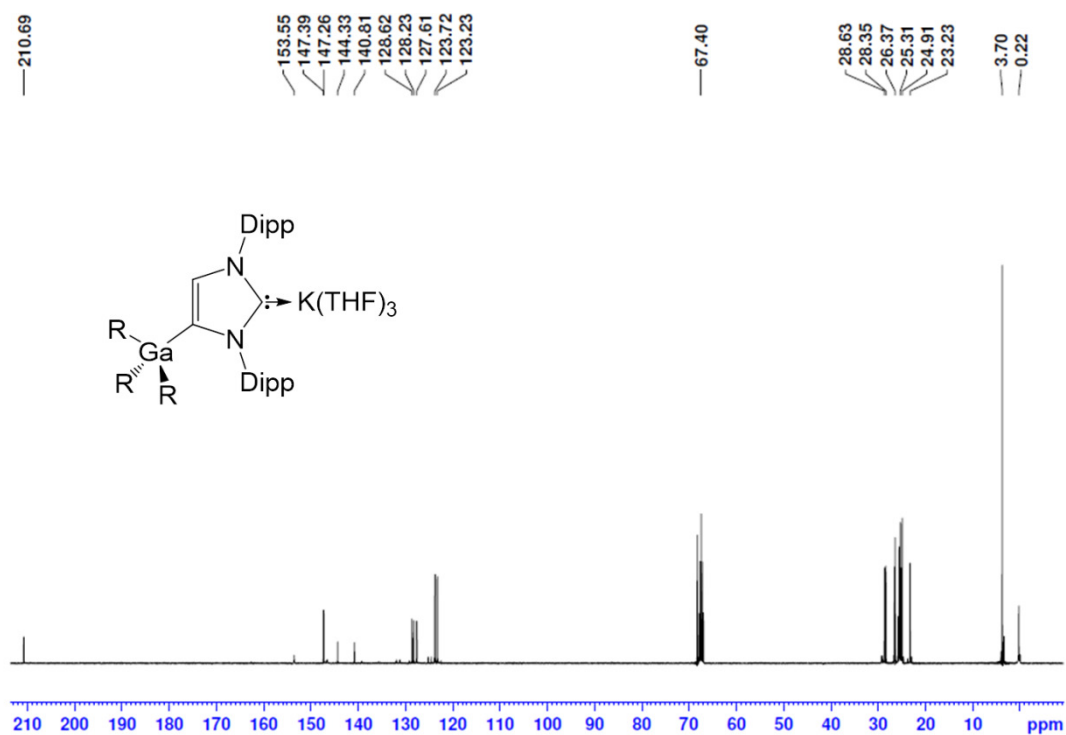


Figure S8: ^{13}C NMR spectrum of **2** in d_8 -THF.

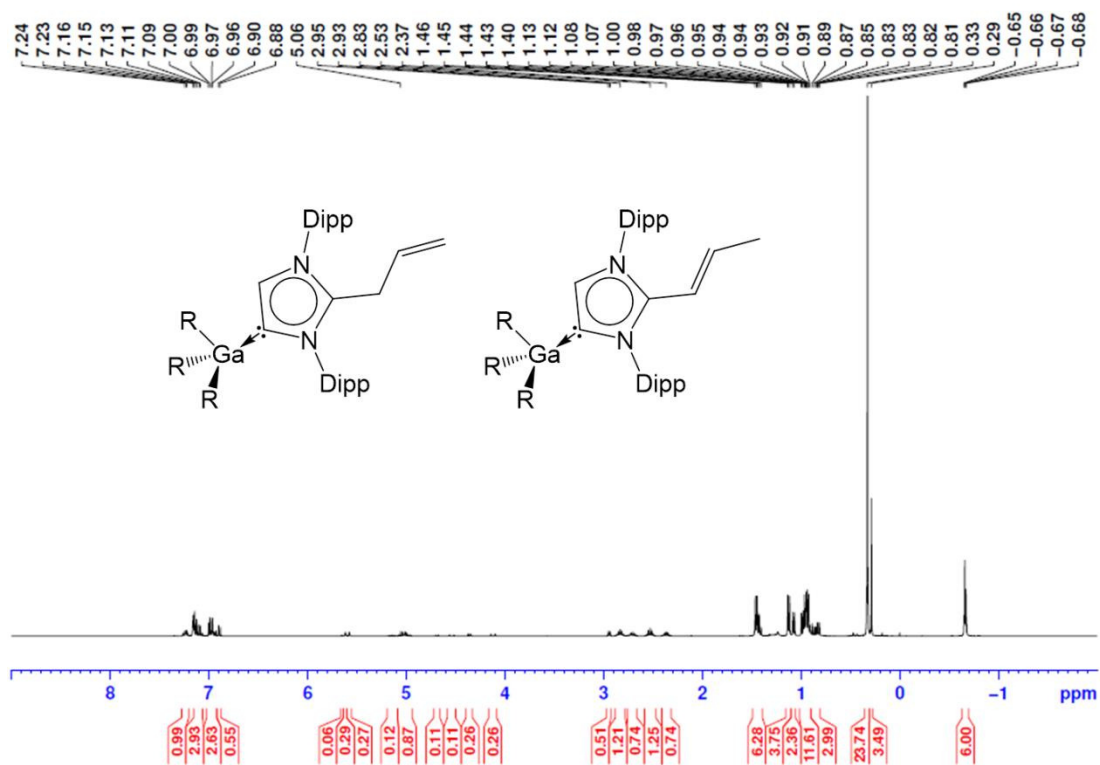


Figure S9: ^1H NMR spectrum of **3** in C_6D_6 .

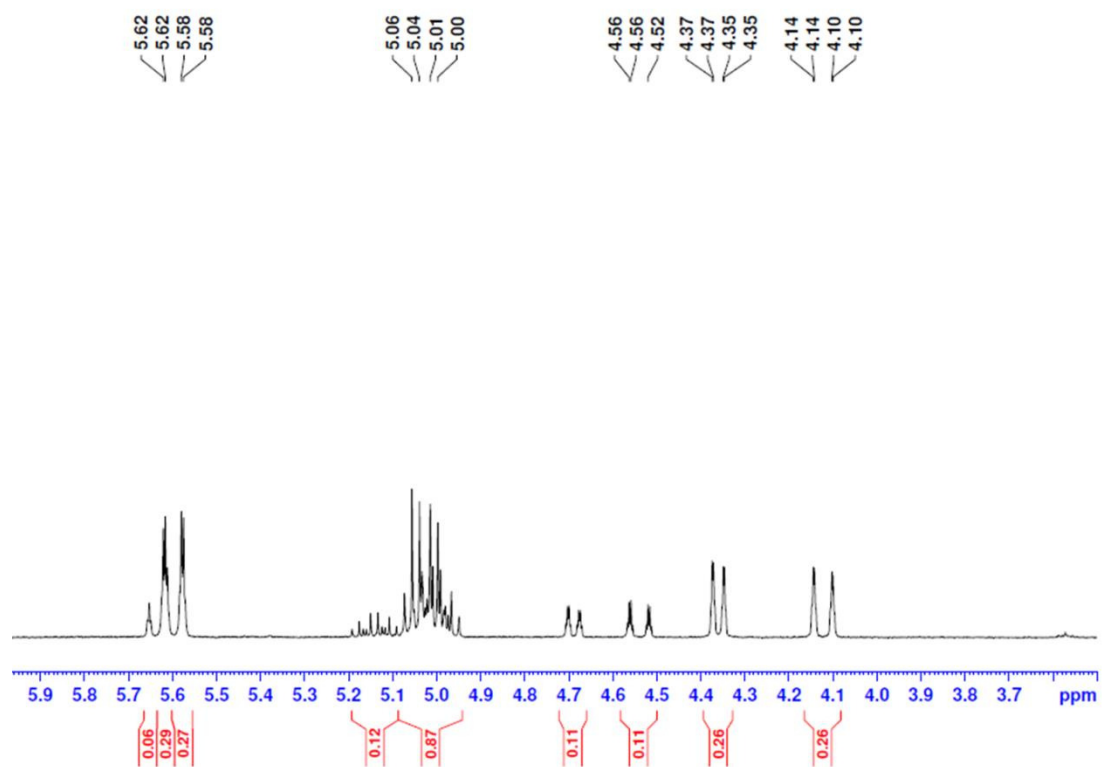


Figure S10: Partial ^1H NMR spectrum of **3** (6 ppm -3.5 ppm region) in C_6D_6 .

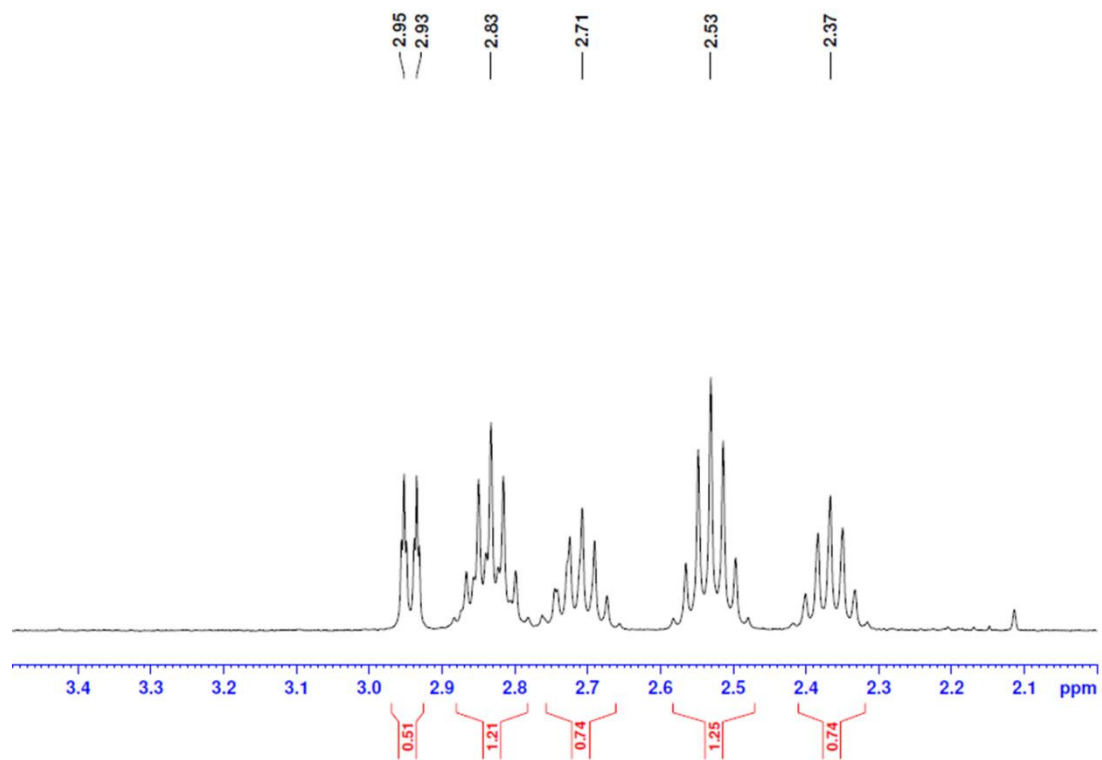


Figure S11: Partial ^1H NMR spectrum of **3** (3.5 ppm -2 ppm region) in C_6D_6 .

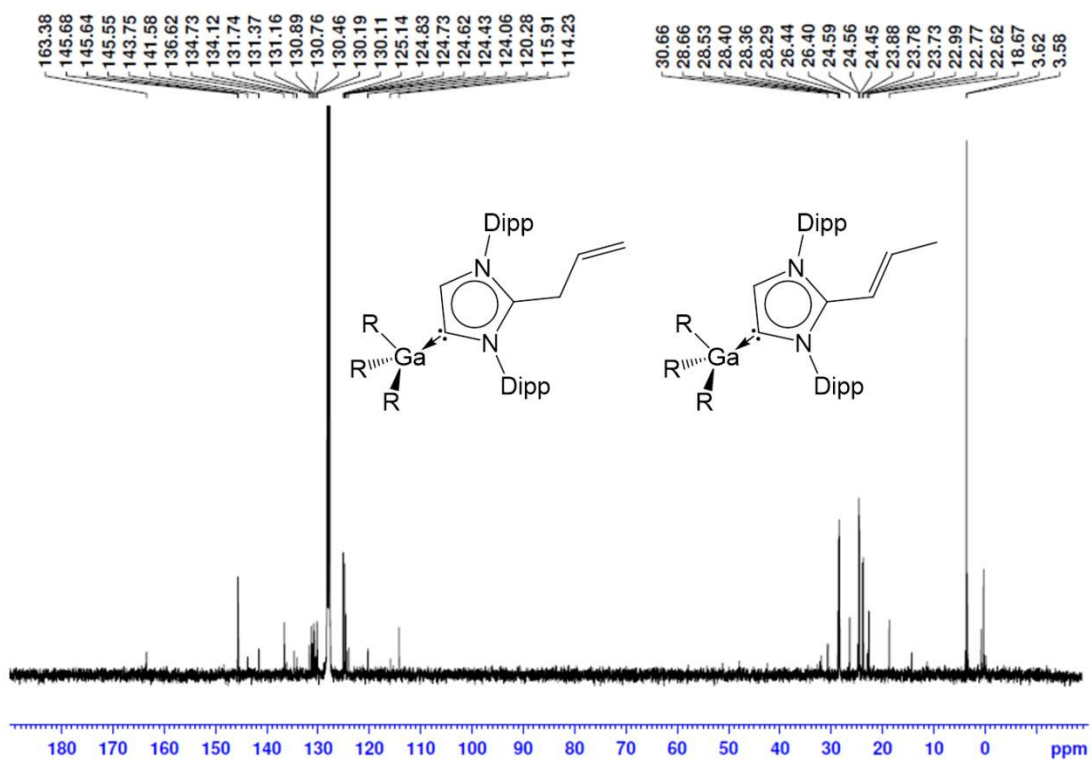


Figure S12: ^{13}C NMR spectrum of **3** in C_6D_6 .

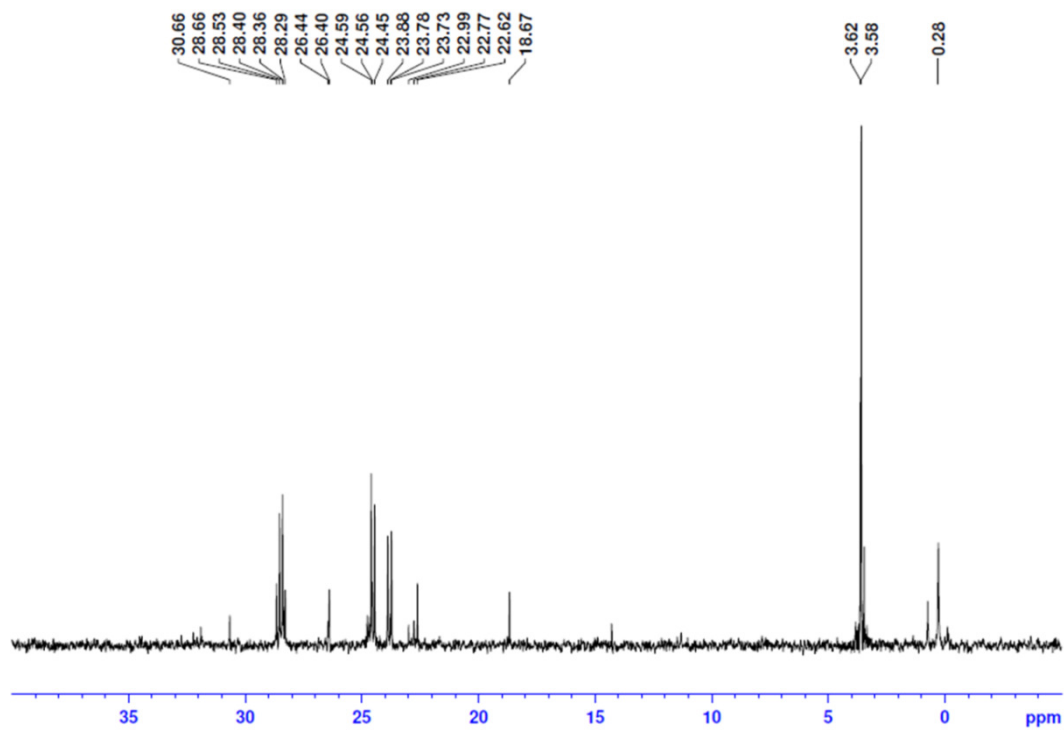


Figure S13: High field region of ^{13}C NMR spectrum of **3** in C_6D_6 .

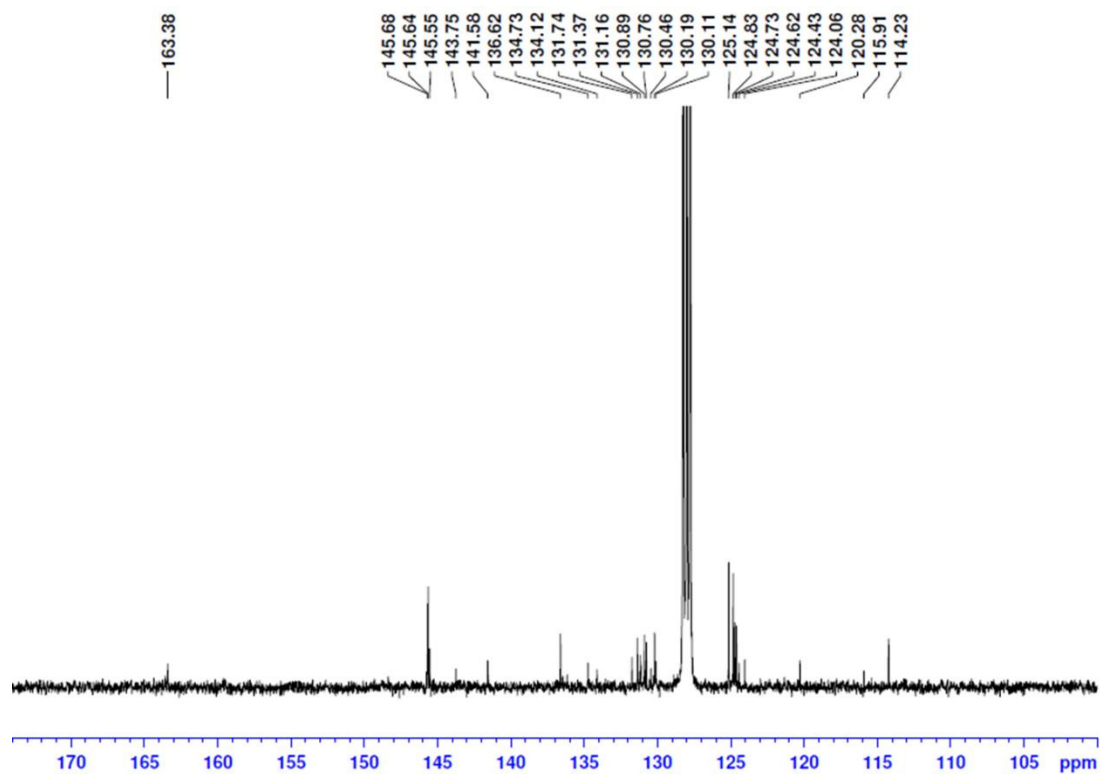


Figure S14: Low field region of ^{13}C NMR spectrum of **3** in C_6D_6 .

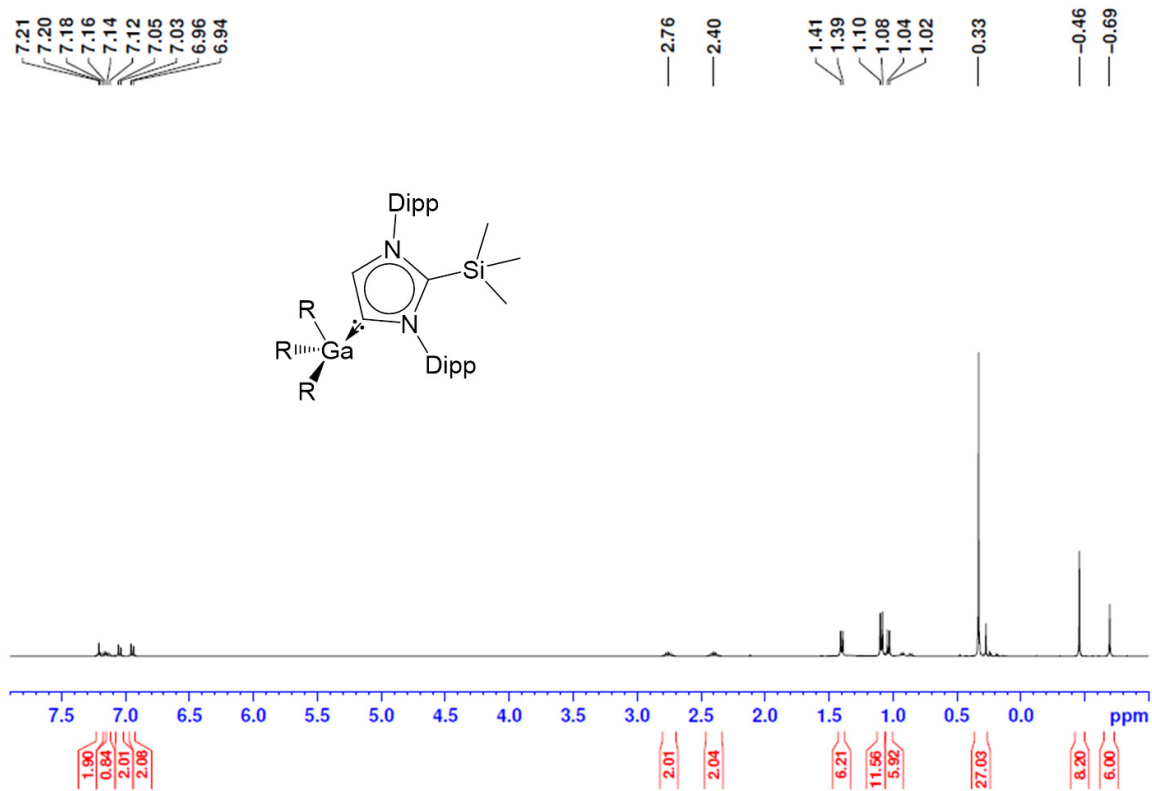


Figure S15: ^1H NMR spectrum of **4** in C_6D_6 .

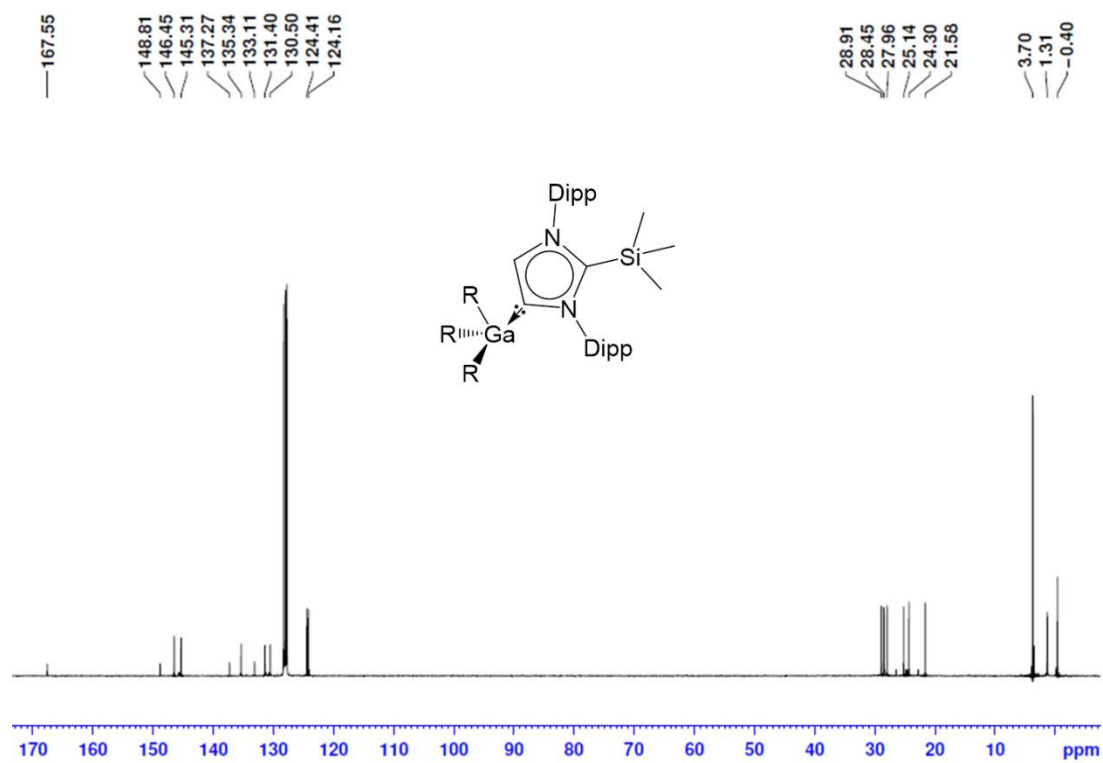


Figure S16: ^{13}C NMR spectrum of **4** in C_6D_6 .